

Quantitative Three-Dimensional Low-Speed Wake Surveys

by
G. W. Brune*

Boeing Commercial Airplane Group
Seattle, Washington 98124

N 93 • 27447
50-027
160480

P-13

Summary

Theoretical and practical aspects of conducting three-dimensional wake measurements in large wind tunnels are reviewed with emphasis on applications in low-speed aerodynamics. Such quantitative wake surveys furnish separate values for the components of drag such as profile drag and induced drag but also measure lift without the use of a balance. In addition to global data, details of the wake flowfield as well as spanwise distributions of lift and drag are obtained. The paper demonstrates the value of this measurement technique using data from wake measurements conducted by Boeing on a variety of low-speed configurations including the complex high-lift system of a transport aircraft.

Nomenclature

b	model span
c	local wing chord
C_D	total drag coefficient
C_{D_i}	induced drag coefficient
c_{d_i}	wing section induced drag coefficient
C_{D_p}	profile drag coefficient
c_{d_p}	wing section profile drag coefficient
C_L	total lift coefficient
c_l	wing section lift coefficient
M	Mach number
p	static pressure
p_t	total pressure
q	dynamic pressure
Re	Reynolds number
S	tunnel cross-section area
U	axial velocity component
V,W	crossflow velocity components
y,z	Cartesian coordinates in measuring plane
α	angle of attack
ΔC_D	upsweep drag
Φ	velocity potential, equation 11
ρ	density
σ	source, equation 9

ξ axial component of vorticity, equation 8
 Ψ stream function, equation 10

Subscripts

ft value per foot
MAC mean aerodynamic chord
ref reference condition
 ∞ freestream values

Introduction

Qualitative wake surveys employing wake imaging (ref. 1) have verified that most aerodynamic flows of interest are stable. Moreover, they can be surveyed economically in large wind tunnels using mechanical traversers and pneumatic probes. Qualitative wake surveys are conducted to visualize the flowfield, which is a prerequisite to a better understanding of aerodynamic performance.

Quantitative three-dimensional wake surveys are a natural extension of wake imaging. They allow separate measurements of profile drag, induced drag, and lift including spanwise distributions. However, there are significant differences in data acquisition and processing between wake imaging and quantitative wake surveys. The latter requires the use of a pneumatic probe with multiple holes instead of a single total pressure probe to record pressures and velocities which can then be converted into aerodynamic forces. Furthermore, quantitative wake surveys require very accurate probe position measurements since spatial derivatives of flow velocities must be computed during data reduction.

Quantitative wake surveys are of much value to the aerodynamic design of airplanes for the following reasons:

- a. They can be used as a diagnostic tool during airplane

* Principal Engineer, Aerodynamics Engineering
Copyright retained by The Boeing Company, 1991.

development to study the effect of configuration changes on the components of drag.

- b. Separate measurements of induced drag and profile drag facilitate the prediction of flight drag based on measurements at low Reynolds number wind tunnel test conditions. This is because induced drag and profile drag are associated with different flow phenomena which must be scaled differently to account for changing Reynolds number.
- c. Separate measurements of the components of drag are also of value to the developer of CFD codes since profile drag and induced drag are usually predicted with different aerodynamic flow models that must be validated separately.

This paper describes the wake survey technique in use at the Boeing Aerodynamics Laboratory which is based on the work of Maskell and Betz. The underlying theory for the measurement of induced drag and lift had been published by Maskell (ref. 2), who also conducted an exploratory wind tunnel test confirming the validity of his method. The theory for the measurement of profile drag is that of Betz (refs. 3, 4). Briefly, model drag and lift can be written as integrals of flow velocities and total pressure, as is well known from basic aerodynamic principles. However, a straightforward application of these equations would not be practical since all three components of velocity would have to be measured throughout the wind tunnel test section. The basic approach employed by Maskell and Betz was to rewrite the drag integrals in terms of flow variables that vanish outside the viscous wake, thereby limiting the wake measurements to a small part of the flowfield. Maskell expressed the main contribution to the induced drag integral in terms of the streamwise component of vorticity, whereas Betz limited the profile drag integration to the viscous wake by introducing an artificial streamwise velocity. This opened the door for practical applications of quantitative three-dimensional wake surveys.

The wake survey methodology in use at Boeing also includes certain features of the work of others. Among them are Hackett and Wu (refs. 5, 6, and 7), who contributed to the theoretical foundation and developed a practical wake survey method with emphasis on applications in automotive engineering.

Several other experimentalists reported quantitative wake surveys. Onorato et al. (ref. 8) conducted wake measurements behind models of automobiles, but their drag analysis does not utilize the simplifications introduced by Maskell and Betz. Chometon and Laurent (ref. 9) performed wake measurements

on a simple wing to investigate the relation between induced drag and vortex drag. Weston of NASA Langley (ref. 10) conducted quantitative wake surveys behind wing half models based on the theory of Maskell and Betz. In his data analysis, Weston focused on the role of vortex cores and modified the definitions of profile drag and induced drag implementing an earlier proposal of Batchelor (ref. 11). El-Ramly and Rainbird published a number of papers (refs. 12 to 15) describing complete flowfield measurements behind wings from which aerodynamic forces were calculated, but they do not provide details of their theoretical analysis.

Wakes of two-dimensional airfoils have been routinely measured for many years with the primary objective of getting accurate profile drag data that cannot be obtained from balances. Wake surveys of three-dimensional configurations have occasionally been conducted but are not widely accepted by design aerodynamicists. The main reason for this is a legitimate concern about the cost of such wake measurements that require the measurement of a large number of data points. This can indeed be a time-consuming and, hence, expensive process if methods that work so well in two-dimensional wake surveys are applied without further refinements. In addition, three-dimensional wake surveys were suspected to be inaccurate since the desired drag and lift values are the composites of a large number of individual measurements. This paper addresses these and other issues and reports on the progress made since Maskell conducted the first wind tunnel test of this kind at the Royal Aircraft Establishment in the U.K. some 20 years ago.

Theory

Assumptions

Aerodynamic forces are calculated from the measured wake flow data assuming:

- a. Wake flow data are measured in a single plane downstream of the model. This plane, located at the so-called wake survey station (fig. 1), is assumed to be perpendicular to the wind tunnel axis. In most wind tunnels, the wake survey station must be moved very close to the model because of test section and hardware limitations.
- b. The flow at the wake survey station is steady and incompressible, which limits the freestream Mach number in the wind tunnel to about 0.5. This does not turn out to be a serious limitation, as will be discussed later.

- c. The flow in the empty wind tunnel is a uniform freestream parallel to the tunnel axis. Any deviations from this ideal wind tunnel, as well as instrumentation misalignments, are assumed to be accounted for by measurements at the wake survey station with the model and its support apparatus removed.
- d. The effective ceiling, floor, and side walls of the empty wind tunnel, defined as the geometric walls modified by the displacement thickness of the wall boundary layers developing in the empty tunnel, are such that the tunnel freestream velocity is everywhere tangent to these surfaces. Note that the presence of a model, particularly a model that is large compared to the test section size, will disturb this displacement surface. Also notice that this choice neglects the possible effect of an axial pressure gradient in the empty tunnel (buoyancy).
- e. Viscous shear stresses at the wake survey station are neglected.
- f. As written, the equations do not account for blowing or suction through the model surface but could easily be modified.

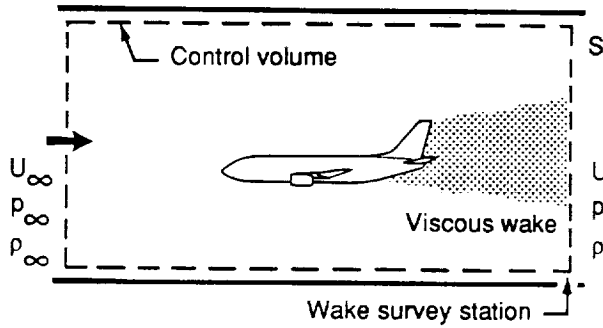


Figure 1. Control Volume for Derivation of Wake Equations

Components of Drag

With these assumptions, an application of the momentum integral theorem, employing the control volume shown in figure 1, provides the following equation for model drag

$$D = \iint_{wake} (p_{t\infty} - p_t) ds + \frac{\rho}{2} \iint_S (V^2 + W^2) ds + \frac{\rho}{2} \iint_S (U_\infty^2 - U^2) ds \quad (1)$$

in which the symbol p_t denotes total pressure and V, W are the components of the crossflow velocity in the

measuring plane perpendicular to the tunnel axis (fig. 2). U and ρ denote the velocity in the direction of the tunnel axis and density, respectively. Undisturbed freestream values are indicated by the subscript ∞ .

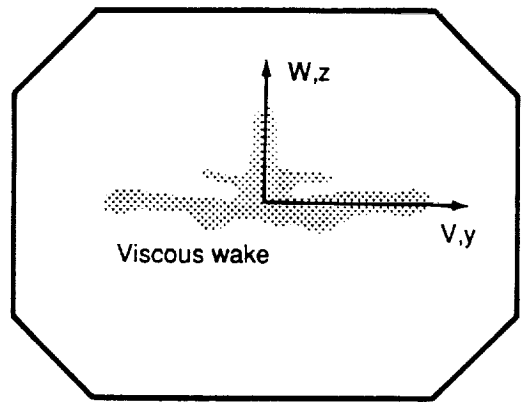


Figure 2. Crossflow Notation

Here, the first term is an integral of the total pressure deficit that is sometimes used as a measure for profile drag even though it is not the only contribution to this type of drag. As indicated, this integral is limited to the viscous wake since the total pressure deficit is zero outside this region of the flow. The second term, representing the kinetic energy of the crossflow, is called vortex drag whereas the third term containing axial velocities does not have any particular name in traditional nomenclature. We will see below that this third term contains contributions to both profile drag and induced drag.

It should be emphasized that equation 1 is valid for configurations in locally compressible flow since the assumption of incompressible flow has only been applied to simplify the velocity and pressure terms at the wake survey station and far ahead of the model.

Equation 1 is not well suited for use in a practical wake measurement technique since only the first integral is limited to the viscous part of the wake. An evaluation of the other two terms would require the measurement of all three velocity components throughout the tunnel cross-section area S .

In order to obtain an equation for profile drag that is suitable for practical wake measurements, Betz (ref. 4) introduced an artificial axial velocity, U^* , defined by the equation

$$U^{*2} = U^2 + \frac{2}{\rho} (p_{t\infty} - p_t) \quad (2)$$

Notice that U^* is the same as the true axial velocity U outside the viscous wake, where the total pressure is $p_{t\infty}$. If one also introduces a perturbation velocity, defined by $u' = U^* - U_\infty$, drag can be written as the sum of profile drag D_p and induced drag D_i ,

$$D = D_p + D_i \quad (3)$$

with

$$D_p = \iint_{wake} [p_{t\infty} - p_t + \frac{\rho}{2}(U^* - U)(U^* + U - 2U_\infty)] ds \quad (4)$$

$$D_i = \frac{\rho}{2} \iint_{wake} (V^2 + W^2 - u'^2) ds \quad (5)$$

The measurement of profile drag can now be conducted economically by measuring total pressure deficit and axial velocity in the viscous wake only.

Motivated by the need to also limit the measurement of induced drag to the viscous part of the wake, Maskell (ref. 2) interpreted the axial velocity perturbation term in equation 5 as a blockage correction in which blockage velocity is calculated from

$$u_b = \frac{1}{2S} \iint_{wake} (U^* - U) ds \quad (6)$$

This blockage correction can easily be implemented by replacing the tunnel freestream velocity in the profile drag equation by an effective freestream velocity, $U_e = U_\infty + u_b$.

The elimination of the u' -term from the induced drag equation is the most questionable aspect of Maskell's theory since the distinction between vortex drag and induced drag disappears. In principle, the u' -term should remain part of induced drag even though it is probably small compared to vortex drag in many applications (ref.16).

Induced Drag

According to Maskell, the remainder of the induced drag equation can be approximated by

$$D_i = \frac{\rho}{2} \iint_{wake} \Psi \xi ds - \frac{\rho}{2} \iint_S \Phi \sigma ds \quad (7)$$

where the symbol ξ represents the component of wake vorticity in the direction of the tunnel axis, referred to below as axial component of vorticity, σ is the crossflow divergence or source. They are calculated from the measured crossflow velocities V, W using the definitions

$$\xi = \frac{\partial W}{\partial y} - \frac{\partial V}{\partial z} \quad (8)$$

$$\sigma = \frac{\partial V}{\partial y} + \frac{\partial W}{\partial z} = -\frac{\partial U}{\partial x} \quad (9)$$

The symbol Ψ is the stream function obtained from a solution of

$$\frac{\partial^2 \Psi}{\partial y^2} + \frac{\partial^2 \Psi}{\partial z^2} = -\xi \quad (10)$$

It describes a flowfield that is induced by the axial component of vorticity. Equation 10 must satisfy the boundary condition $\Psi = 0$ at the tunnel walls so that they become a streamline of this two-dimensional flowfield.

The symbol Φ denotes a velocity potential calculated from

$$\frac{\partial^2 \Phi}{\partial y^2} + \frac{\partial^2 \Phi}{\partial z^2} = \sigma \quad (11)$$

and the following boundary condition of no flow through the tunnel walls

$$\frac{\partial \Phi}{\partial n} = 0$$

Notice that the first integral in equation 7 is limited to the viscous wake since vorticity vanishes outside. The second term would still require measurements throughout the test section area but wake measurements behind models of airplane configurations have shown that the source σ is negligibly small outside the viscous wake. Hence, induced drag can be approximated by

$$D_i \approx \frac{\rho}{2} \iint_{wake} (\Psi \xi - \Phi \sigma) ds \quad (12)$$

Lift

The momentum integral theorem together with the control volume of figure 1 yields the following equation for lift

$$L = \iint_{S_4} p ds - \iint_{S_3} p ds - \rho \iint_S W U ds \quad (13)$$

where the first two terms represent the difference in static pressure between tunnel floor and ceiling. This integration is performed along upper and lower surfaces of the control volume, denoted respectively by S_3 and S_4 . The third term arises from the downwash behind the model. The equation for lift can be cast into the following form (refs. 2, 16)

$$L = \rho U_\infty \iint_{wake} y \xi ds + \rho \iint_S (U_\infty - U) W ds \quad (14)$$

in which the first integral is expressed in terms of axial vorticity that vanishes outside the viscous wake and, hence, only requires measurements in the wake. In most cases the second integral is expected to be small so that lift can be approximated by

$$L \approx \rho U_\infty \iint_{\text{wake}} \gamma \xi ds \quad (15)$$

Instrumentation

Five-Hole Probe

Most three-dimensional wake surveys conducted by Boeing employ pneumatic probes with multiple orifices mounted on mechanical traversers. All wake survey tests described in this paper used a single five-hole conical probe 0.25 inches in diameter (fig. 3) in a fixed position or nonnulling mode for fast data acquisition. Rakes of pneumatic probes have been considered in order to shorten data acquisition time but were discarded to avoid the increased data handling complexity associated with their use and possible mutual probe interference. Pneumatic probes have the following advantages for testing in large low-speed wind tunnels:

- a. They can accurately and simultaneously measure all three components of wake velocity and total pressure.
- b. They provide time averages of data, thereby limiting the data volume and data processing time.
- c. They are rugged and not easily contaminated by dirt in the tunnel circuit.

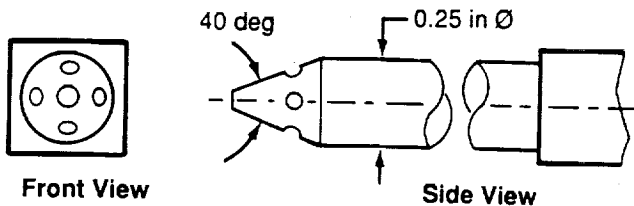


Figure 3. Five-Hole Probe Geometry

These features are not shared by most data acquisition systems developed for experiments in small research facilities. However, the probes and the mechanical traversers on which they are mounted are intrusive and will disturb the flow to some degree. Under certain conditions, intrusive probes are known to cause meandering of the vortex in which they are inserted and make the vortex core appear larger than its true size (ref.17). Perhaps an

even greater concern in using such measuring systems is the flow disturbance due to the traverser, which can cause significant perturbations of model lift and drag. These potential problems represent a great challenge to the experimentalist who must achieve a workable compromise between the rigidity of the measuring system and its intrusiveness.

Probe Calibration

Probes are calibrated by placing them at selected pitch and yaw angles in a flow of known total and static pressures (ref. 18). This provides calibration curves for the deviation between true and indicated values of total pressure measured by the center hole of the five-hole probe as a function of flow angle, probe design, and Reynolds number based on probe size. Furthermore, this procedure relates flow angles and velocity components to pressures measured by the orifices on the side faces of a multiple hole probe, and also furnishes static pressure.

Mechanical Traverser

Most wake survey tests conducted by Boeing utilize vertical traversing struts that are a permanent part of the wind tunnel test section equipment. Sometimes an additional mechanical traverser is mounted on this strut to move the probe in a lateral direction while the strut traverses the vertical direction. Employing the wind tunnel strut usually simplifies the test setup, but requires compensation for the mechanical backlash of the strut.

All wake measurements discussed in this paper used traversers that move the probe parallel to the tunnel side walls, providing data points arranged in a Cartesian grid. Work is in progress on improved traversers that move the probe along circular arcs while the wind tunnel strut, on which the traverser is mounted, is temporarily at rest (fig. 4). These second generation traversers are less intrusive and are computer controlled, which simplifies data acquisition. However, the task of aligning the probe with the wind tunnel axis during the entire wake survey becomes very difficult. A probe that is not aligned well with the tunnel axis will measure crossflow velocities and a corresponding apparent wake vorticity that are partially due to probe misalignment. One can account for this probe misalignment by mapping the flow in the empty tunnel at the same location where wake surveys are normally conducted. The measured empty tunnel crossflow velocities are then used to compute a correction to the final drag and lift data. Notice, however, that empty tunnel surveys need not be conducted to determine the flow qualities of a tunnel

that are known from earlier calibration tests.

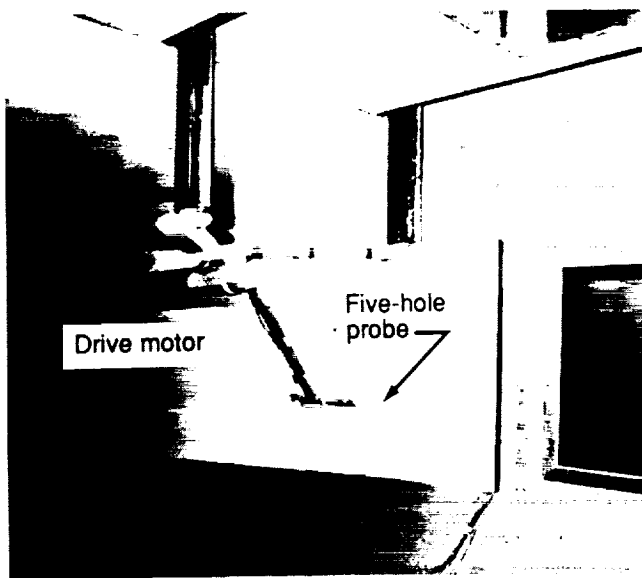


Figure 4. Mechanical Traverser in Empty University of Washington Wind Tunnel

Data Reduction

In the usual procedure, the five-hole probe measures total pressure deficit and all three components of wake velocity at a large number of points, normally in excess of 10,000. Handling this data volume in a timely fashion is the most difficult aspect of the data reduction procedure. Basically, the procedure consists of two steps: A review of the data for erroneous and duplicate data sets, and the calculation of lift and drag from the final data set.

The calculation of profile drag using equation 4 is straightforward and only requires integration. The calculation of induced drag and lift using equations 12 and 15 is more difficult since vorticity and source strength must be computed as intermediate results. These calculations require numerical differentiation of measured crossflow velocity components, V and W , which can easily lead to erroneous values of induced drag and lift if not done properly. Numerical experimentation with various schemes showed that accurate vorticity and source data could be calculated by fitting cubic splines to the measured crossflow velocities.

In order to obtain the stream function Ψ and the velocity potential Φ from equations 10 and 11, the computational domain is extended with uniform grid spacing from the wake survey region to the walls of the wind tunnel. Where necessary, fillets in the corners of the test section are neglected. Values of axial vorticity and source strength are prescribed throughout the computational domain,

which are in general nonzero in the wake survey region and zero outside. A fast Poisson solver of the FISHPAK library (ref. 19) provides solutions for Ψ and Φ . Since the total number of grid points necessary for the calculation frequently exceeds 200,000, the use of a supercomputer is required for this phase of the data reduction. Software for this purpose has been developed at Boeing.

Standard correction methods (ref. 20) are applied to lift and drag obtained from wake surveys to account for the effects of wind tunnel walls. The effect of model support struts is accounted for by including part of the model support wake during wake surveys. Most support struts shed very little axial vorticity since they are designed to minimize the disturbance of the circulation around the model. Hence, their presence is primarily visible in the spanwise distribution of profile drag and not in the spanwise data of induced drag or lift. Assuming a spanwise variation of profile drag that might exist in the absence of the strut, profile drag can then be corrected.

Since wake surveys are time-consuming and some low-speed wind tunnels are not equipped with a heat exchanger to control temperature, profile drag must sometimes be corrected for the effect of temperature increases with time.

Wake Survey Test Results

Three tests are described, ranging in complexity from measurements behind a simple wing to a wing-body-nacelle combination in high-lift configuration. They illustrate the practical aspects of quantitative wake measurements such as model installation, data acquisition, test procedure, and provide examples of the type and quality of data obtained from wake surveys. Each of these tests has unique features dictated by different test objectives, type and availability of model and wind tunnel, and testing budget. All tests used basically the same data acquisition system and data reduction procedure but different hardware.

High-Lift Test of Transport Aircraft

A large half model of a twin engine transport was tested at Mach 0.22 and 1.4 million chord Reynolds number in the Boeing Transonic Wind Tunnel (fig. 5). The tunnel features an 8-by 12-ft test section with slotted walls. The wing was in high-lift configuration with take-off flaps deployed. The model had a half-span of 52 inches and was installed vertically above a horizontal splitter plate. Two different engine simulations were employed including a flowthrough nacelle and a turbo-powered simulator

(TPS). The purpose of this experiment was to determine the feasibility of making quantitative wake surveys using models of realistic high-lift configurations.

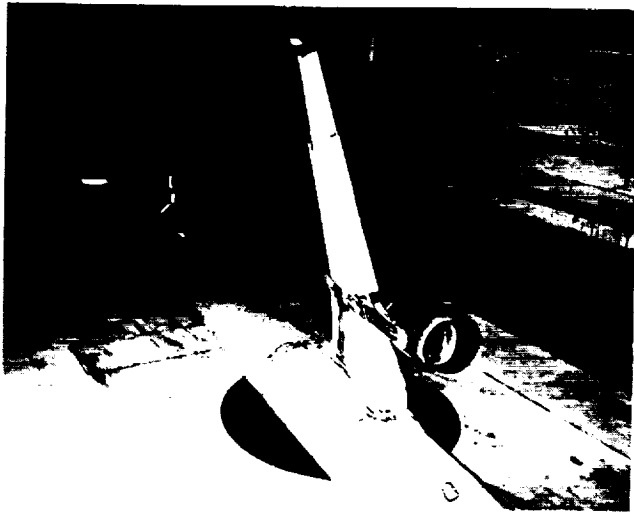


Figure 5. High-Lift Half-Model in Boeing Transonic Wind Tunnel

Wake surveys were conducted in a plane two mean aerodynamic chord lengths (24 inches) downstream of the inboard wing trailing edge, which was as far downstream as test section and data acquisition hardware permitted. The boundaries of the wake survey region (fig. 6) were chosen to capture wing and nacelle wakes but did not include the wake behind the fuselage.

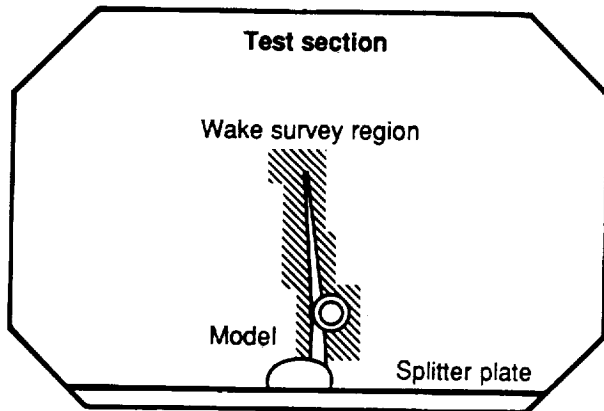


Figure 6. Example of Wake Survey Region

Wake surveys are time-consuming since a large number of data points must be taken to adequately describe the wake. In this case measurements had to be performed at about 15,000 wake points. In order to complete a wake survey within a reasonable time of about 2 hours, data were recorded while the probe traversed at a fixed speed. Preliminary investigations in which the traversing speed was varied showed that this mode of testing produced accurate data up to a probe speed of 1 inch per second.

Measured velocities of the crossflow perpendicular to the tunnel axis were converted into axial vorticity as described above. Such vorticity data together with the measured total pressure deficit provides much insight into the structure of wing wakes. Figures 7 and 8 show contour plots of these data for the model with two different engine representations. Wind tunnel test conditions and model geometry are the same for both sets of data. The wake flows are shown in airplane view with the wing tip vortex of the right wing on the right side of the plots. The nacelle region is visible on the left side of each plot. Inboard total pressure and vorticity contours are quite different for the two nacelle configurations with the TPS data indicating the extent of the powered jet. However, the outboard contours, including the tip vortex and the powerful vortex to the left of the tip vortex, shed from the outer edge of the trailing edge flap, are almost identical for the two wakes.

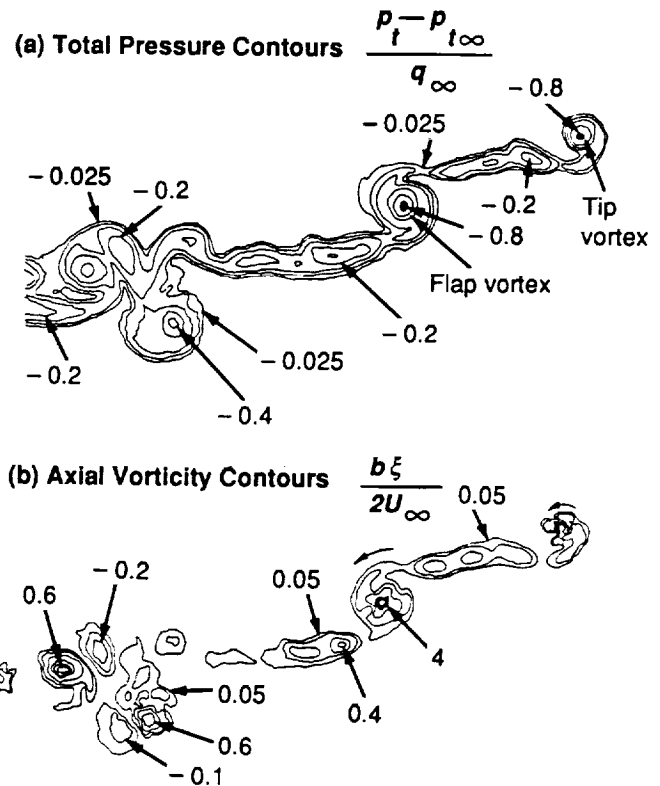


Figure 7. Wake Flow Data of Transport High-Lift Model With Flowthrough Nacelles

Wake flow data provide important qualitative information during airplane design but are also useful for the validation of CFD codes. An example of the latter is given in figure 9 where the total pressure contours of figure 7 are compared with wake rollup predictions obtained from A502/PANAIR (ref. 21) for this high-lift airplane configuration with flowthrough nacelle.

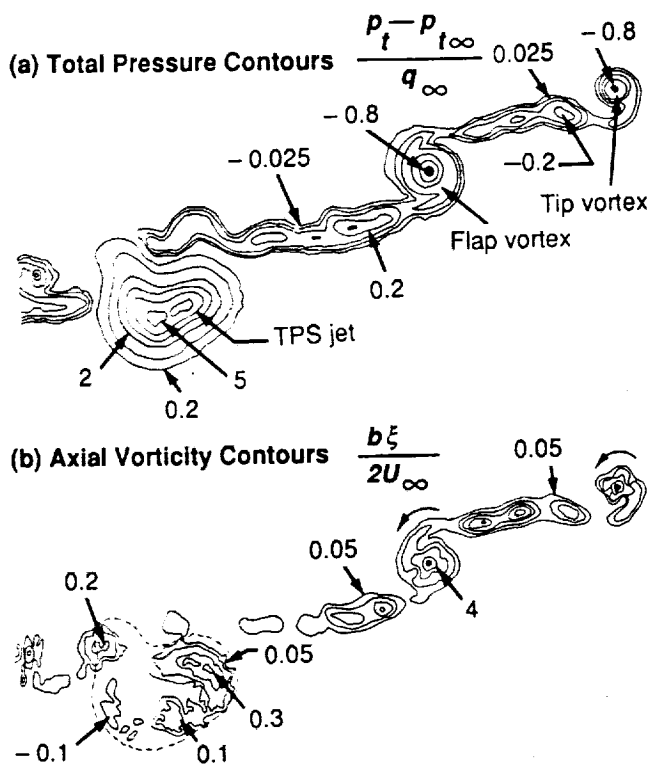
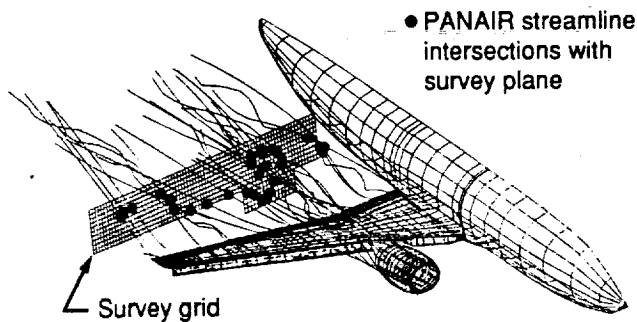
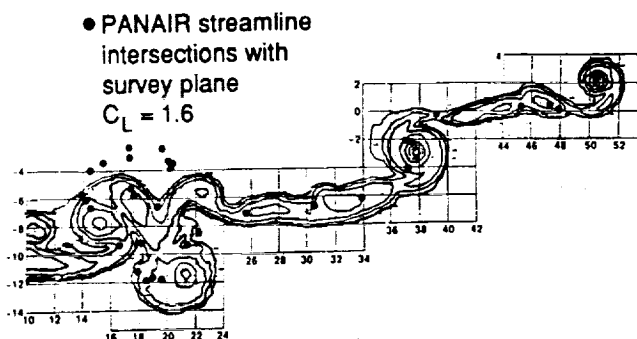


Figure 8. Wake Flow Data of Transport High-Lift Model With Turbo-Powered Simulator (TPS) Powered Nacelles

(a) Panel Model and Streamline Calculations



(b) Streamline Intersections With Survey Plane



Total pressure wake contours from flowthrough nacelle test

Figure 9. A502/PANAIR Prediction of Wake Shape of Transport High-Lift Configuration

Spanwise distributions of profile drag and induced drag derived from the wake data of figures 7 and 8 and the corresponding axial velocity data are plotted in figure 10. Spanwise induced drag is defined here as the integral of the integrand of equation 12 in the direction normal to the wing surface, which is different from the usual definition of spanwise induced drag defined as the product of wing section lift and induced angle of attack. As seen in the figure, the major contribution to induced drag arises from the strong tip and flap edge vortices. Profile drag of the model with TPS nacelle includes a large region of negative values representing the thrust of the TPS jet. The two configurations have almost identical distributions of induced drag and profile drag for the outer half of the wing, except that wing and flap vortices from the TPS configuration are shifted slightly outboard, possibly being displaced by the TPS jet. Such good agreement of the outboard data taken at the same angle of attack and behind the same wing geometry demonstrates the excellent repeatability of these measurements. It should be emphasized that the spanwise distributions of drag shown in figure 10 are somewhat distorted because of wake deformations between wing trailing edge and wake survey station. Thus, any comparison of spanwise drag or lift data with data from other sources should be interpreted with caution. However, spanwise wake data frequently reveal the origin of major contributions to drag and lift and are therefore of much value in aerodynamic design.

The vorticity data in the wake of the TPS-powered model were used to calculate wing spanload as described in reference 22. The result is shown in figure 11 together with inviscid theoretical predictions of the A502/PANAIR code. These theoretical data represent a spanwise lift distribution, scaled by the local wing chord and nondimensionalized by the sum of all lift and side forces in the outboard wing and nacelle region. Good agreement is demonstrated outboard of the nacelle. The large differences in the nacelle region are mainly due to sideforces, which, in the wake survey data, could not be distinguished from lift.

Simple Wing Study

The main objective of this test was to learn more about the accuracy and measurement repeatability of quantitative wake surveys (ref. 23). In this test, the wake was mapped behind a simple rectangular wing model that had a span of 6 feet and an untwisted NACA0016 airfoil section. The test was conducted at the University of Washington Aeronautical Laboratory in an 8- by 12-ft low-speed

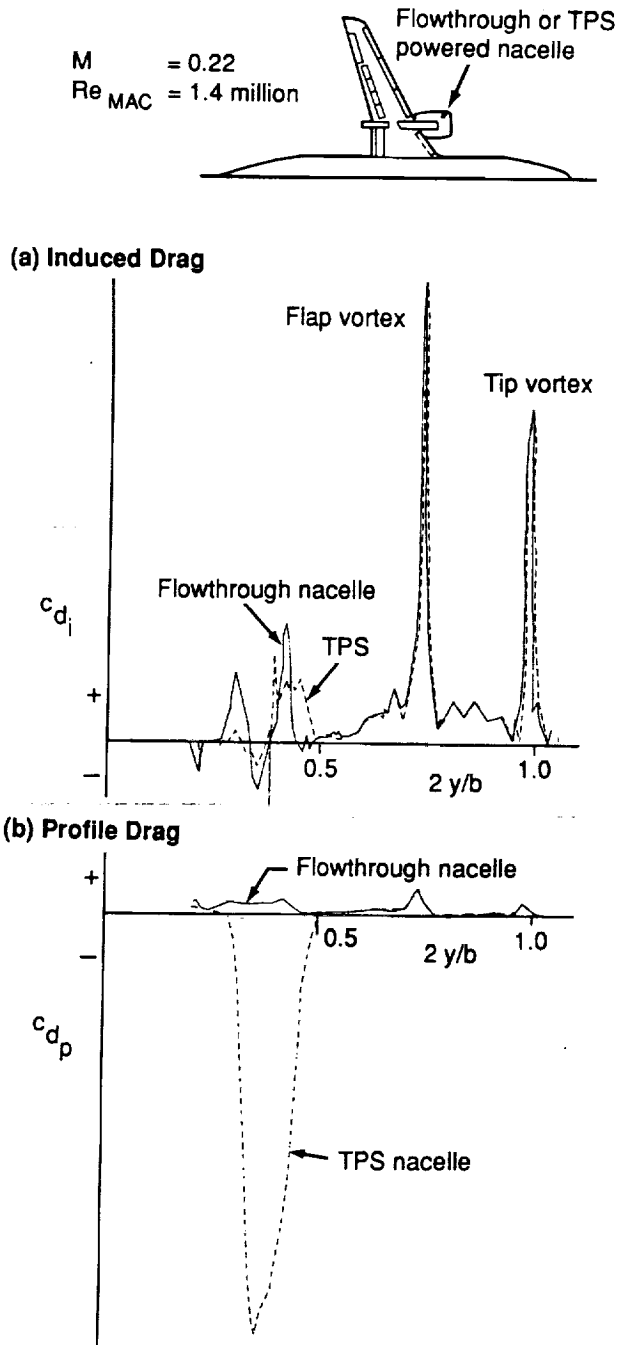


Figure 10. Spanwise Drag Data From Wake Surveys Behind Transport High-Lift Configuration

wind tunnel. All measurements were taken at 0.18 Mach number and 1.27 million chord Reynolds number. The model was installed horizontally at the center of the test section. It was supported by a floor-mounted strut that in turn was mounted on an external balance located below the wind tunnel (fig.12).

Wake surveys were conducted one chord length behind the wing trailing edge and at several angles of attack below stall. A very important purpose of this and other wake tests had been to verify that the

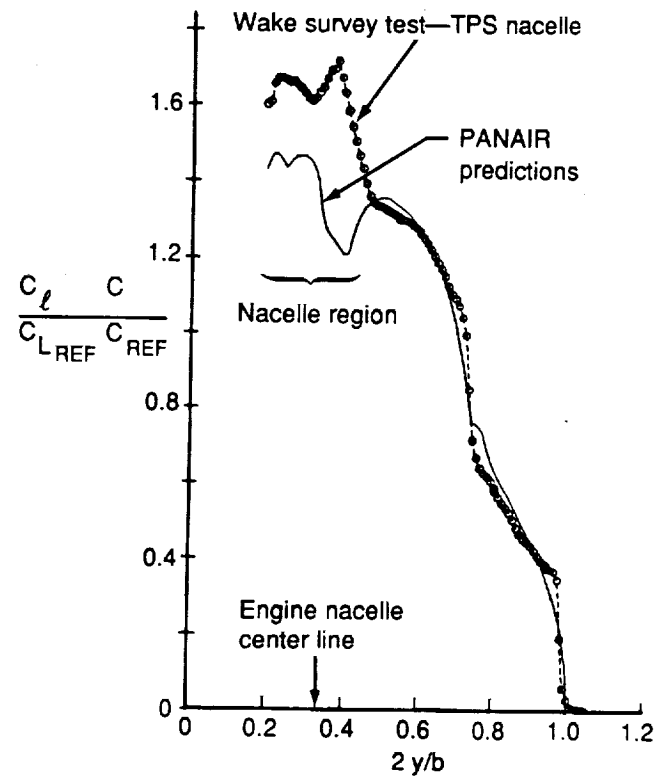
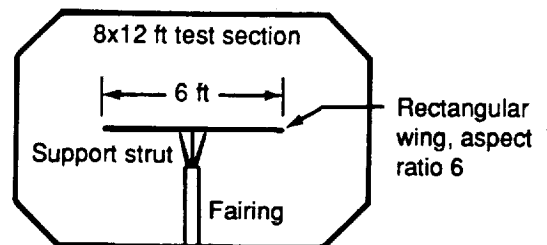


Figure 11. Spanwise Wing Loads of Transport High-Lift Model From Wake Survey and A502 PANAIR Code Prediction

planned quantitative wake survey would indeed capture the wake. This was done by applying the wake imaging technique (ref. 1), which displays total pressure contours measured by the center hole of the five-hole probe. Since viscous wakes can be seen as regions of total pressure loss, the regions in which wakes have to be surveyed can easily be identified.

(a) Front View of Model in Test Section



(b) Side View of Model and Probe Traverser

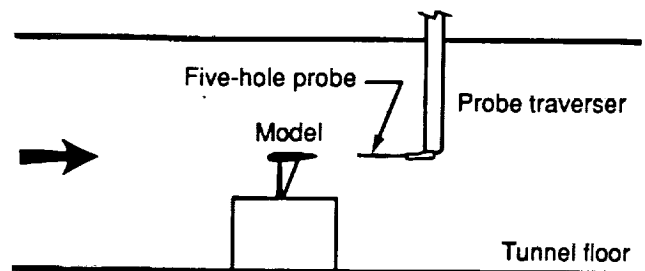


Figure 12. Simple Wing Model in the University of Washington Low-Speed Wind Tunnel

Lift curve and drag polar obtained from wake surveys are compared in figure 13 with corresponding balance data measured during this test. Wake and balance data were recorded at the same test conditions defined by the quoted angles of attack, Mach number and Reynolds number. After the test, both types of data were corrected for wind tunnel wall effects in exactly the same way. The figure also shows the variation of profile drag with lift measured during wake surveys. Excellent agreement of wake and balance data is shown in these figures, providing proof of the high measurement accuracy that can be achieved in quantitative wake surveys.

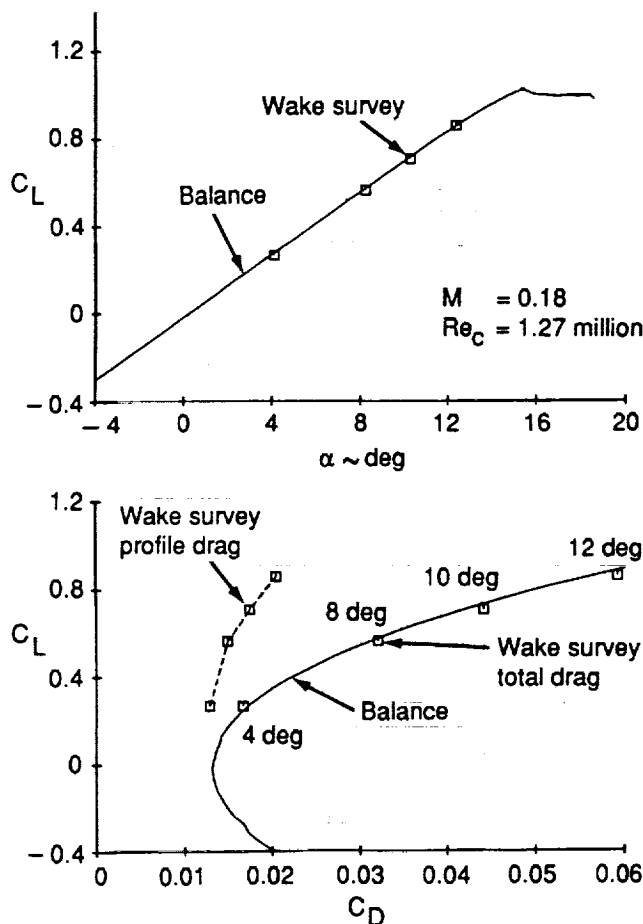


Figure 13. Lift and Drag of Simple Wing From Wake Surveys and Balance

For practical applications, the ability of a wake survey technique to repeat the measurements with very little data scatter is as important as a good absolute measurement accuracy. Figure 14 contains tabulated data for lift and drag components measured in three different wake surveys at the same angle of attack and at the same wake location. These are true repeat runs conducted several days apart. All wake data repeated very well, particularly lift, total drag, and induced drag. Profile drag

scatter is slightly higher than the scatter in the other data. For comparison, figure 14 also contains a table with repeat balance data at the same wind tunnel test conditions.

(a) Wake survey data for $\alpha = 8.22$ deg

Wake survey	C_L	C_D	C_{Dp}	C_{Di}
1	0.5668	0.0323	0.0155	0.0168
2	0.5653	0.0319	0.0148	0.0171
3	0.5651	0.0321	0.0150	0.0171

(b) Balance data for $\alpha = 8.22$ deg

Balance run	C_L	C_D
1	0.5738	0.0319
2	0.5722	0.0318
3	0.5722	0.0319
4	0.5709	0.0319

Figure 14. Wake and Balance Measurement Repeatability

During this wind tunnel experiment, vortex generators were mounted on the model in order to determine the accuracy of wake surveys in measuring drag increments due to configuration changes. Measured total wake drag increments were found to be within one drag count of balance drag increments. Note that this difference is the same as the scatter in the balance drag data (fig. 14). These results not only demonstrated excellent accuracy in measuring wake drag increments, but also provided the increments of profile drag and induced drag associated with the addition of vortex generators.

Aftbody Drag Tests

Wake surveys were conducted with various fuselage models of transport airplanes in order to improve our understanding of aftbody flowfields and the drag associated with them. Contrary to most military transports, civil transports feature moderate aftbody upsweep with a correspondingly smaller contribution to drag. The vortices shed from such aftbodies are relatively weak, but their associated drag must nevertheless be understood when seeking opportunities for airplane drag reduction.

Aftbody drag experiments were carried out in the Boeing Research Wind Tunnel in Seattle at 0.18 Mach number and 1.18 million Reynolds number per foot. In all tests, the fuselage was supported by wing stubs extending through the tunnel side walls that are 5 feet apart (fig. 15). Notice that in this test setup wing lift distribution and, hence, wing induced downwash at the location of the tail were not realistically simulated. The wing tips, in turn, were

mounted on an external balance, situated below the test section. This allowed a comparison of wake survey drag measurements with balance drag.

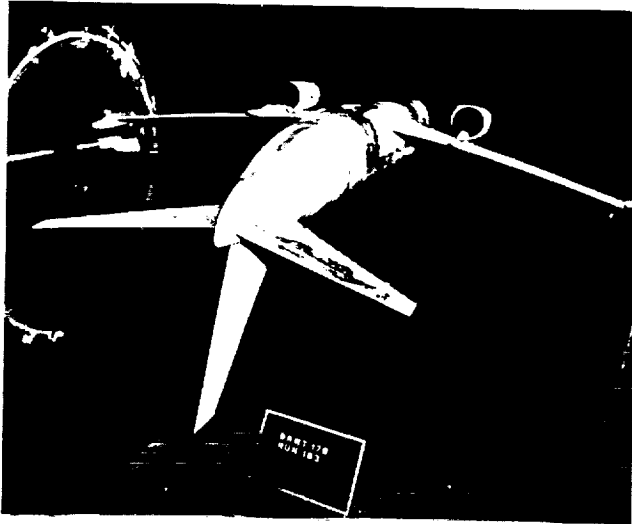


Figure 15. Aftbody Drag Test in Boeing Research Wind Tunnel

Parametric studies investigating the effect of aftbody length and upsweep angle on 7-7 fuselage drag provided quantitative data for vortex drag and profile drag as functions of angle of attack (ref. 24). As shown in the example of figure 16, vortex drag of upswept and symmetric aftbodies of civil transports can be measured in wake surveys with very little data scatter even though aftbody vortex drag is indeed very small.

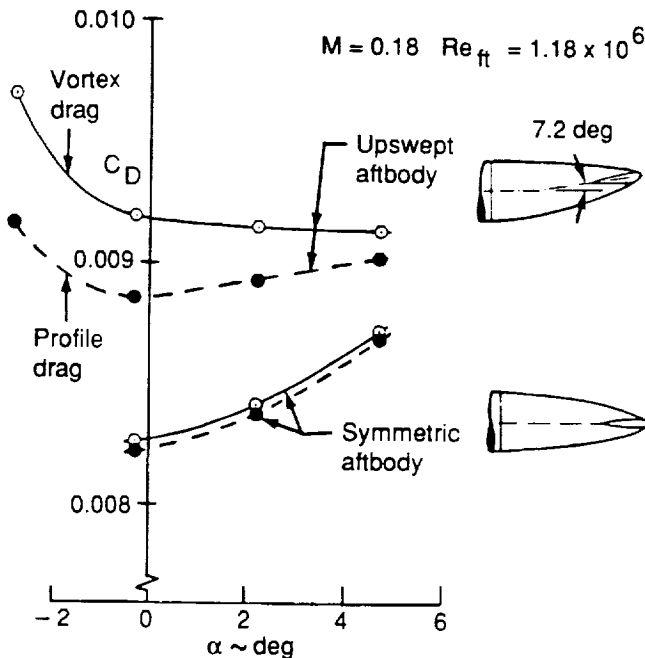


Figure 16. Drag Components of Symmetric and Upswept Aftbody Configurations

Wake measurements of upsweep drag of the 737 are compared in figure 17 with balance data. This kind of drag is defined as the difference in drag between symmetric and upswept aftbodies at the same test condition. As seen, wake drag is well within the uncertainty band of the force measurements providing further demonstration for the accuracy of three-dimensional wake measurements.

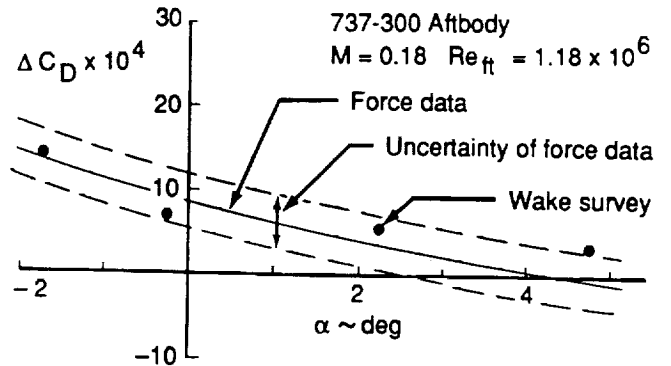


Figure 17. Upsweep Drag From Balance and Wake Surveys

Conclusions

The paper describes the wake survey methodology developed at Boeing for the purpose of measuring the components of drag of low-speed, high-lift configurations. Important elements of this technique including mechanical probe traverser and pneumatic probe design, refinement of the underlying theory, and data reduction procedures are still under development at the present time. However, the technique has already been successfully applied in several wind tunnel tests as shown in this paper. The following valuable features of this measuring technique should be noted:

- a. They provide separate measurements of induced drag, profile drag, and lift.
- b. Measurement accuracy and data repeatability are comparable to balance measurements even though lift and drag data are the composites of a large number of individual measurements.
- c. Small increments in individual components of drag due to minor configuration changes can be measured accurately.
- d. Spanwise distributions of lift can be obtained. This is of value in high-lift aerodynamics since the small flap sizes of most high-lift models make it extremely difficult to measure spanlift data using surface pressure taps. However, all

spanwise wing data measured in wake surveys should be interpreted with caution since they are usually distorted to some degree by wake rollup and, hence, are influenced by practical limitations on the location of the plane in which the survey is conducted.

- e. Wake surveys provide spanwise distributions of profile drag and induced drag, which are of value in diagnosing the effects of local changes to the configuration geometry.
- f. During each wake survey a large number of velocity and pressure data are recorded which can serve as validation data for CFD codes in addition to providing lift and drag data.

Acknowledgements

I would like to acknowledge the technical contributions of my present and former colleagues at Boeing, in particular, Messrs. P. Bogataj, J. Crowder, T. Hallstaff, M. Hudgins, D. Kotker, R. Stoner, and E. Tinoco. I would also like to thank Dr. J. McMasters, and Messrs. M. Mack and K. Moschetti for their review and comments on the draft of this paper.

References

1. Crowder, J. P., "Quick and Easy Flow Field Surveys," *Astronautics and Aeronautics*, November 1980
2. Maskell, E. C., "Progress Towards a Method for the Measurement of the Components of the Drag of a Wing of Finite Span," RAE Technical Report 72232, 1972
3. Schlichting, H., *Boundary-Layer Theory*, 6th ed., McGraw-Hill, 1968
4. Betz, A., "A Method for the Direct Determination of Profile Drag," ZFM, vol. 16, 42, 1925 (in German)
5. Wu, J. C., J. E. Hackett, and D. E. Lilley, "A Generalized Wake-Integral Approach for Drag Determination in Three-Dimensional Flows," AIAA Paper 79-0279, January 1979
6. Hackett, J. E. and J. C. Wu, "Drag Determination and Analysis from Three-Dimensional Wake Measurements," ICAS Paper No. 82-644, August 1982 (text not available)
7. Hackett, J. E. and A. Sugavanam, "Evaluation of a Complete Wake Integral for the Drag of a Car-Like Shape," SAE Paper 840577, February 1984
8. Onorato, M., A. F. Costelli, and A. Garrone, "Drag Measurement Through Wake Analysis," SAE Paper 840302, 1984
9. Chometon, F. and J. Laurent, "Study of Three-Dimensional Separated Flows, Relation between Induced Drag and Vortex Drag," *European Journal of Mechanics, B/Fluids*, vol. 9, No. 5, 1990, pp 437-455
10. Weston, R. P., "Refinement of a Method for Determining the Induced and Profile Drag of a Finite Wing from Detailed Wake Measurements," PhD thesis, University of Florida, 1981
11. Batchelor, G. K., "Axial Flow in Trailing Line Vortices," *Journal of Fluid Mechanics*, vol. 20, part 4, 1964, pp. 645-653
12. El-Ramly, Z., W. J. Rainbird, and D. G. Earl, "Wind Tunnel Measurements of Rolling Moment in a Swept-Wing Vortex Wake," *Journal of Aircraft*, vol. 13, No. 12, December 1976, pp. 962-967
13. El-Ramly, Z. M. and W. J. Rainbird, "Effect of Simulated Jet Engines on the Flowfield behind a Swept-Back Wing," *Journal of Aircraft*, vol. 14, No. 4, April 1977, pp. 1343-1349
14. El-Ramly, Z. M. and W. J. Rainbird, "Computer-Controlled System for the Investigation of the Flow behind Wings," *Journal of Aircraft*, vol. 14, No. 7, July 1977, pp. 668-674
15. El-Ramly, Z. M. and W. J. Rainbird, "Flow Survey of the Vortex Wake behind Wings," *Journal of Aircraft*, vol. 14, No. 11, November 1977, pp. 1102-1108
16. van Dam, C. P., K. Nikfetrat, I. C. Chang, and P.M.H.W. Vijgen, "Drag Calculations of Wings Using Euler Methods," AIAA Paper 91-0338, January 1991
17. Green, S. I. and A. J. Acosta, "Unsteady Flow in Trailing Vortices," *Journal of Fluid Mechanics*, vol. 227, 1991, pp. 107-134
18. Treaster, A. L. and A. M. Yocum, "The Calibration and Application of Five-hole Probes," *ISA Transactions*, vol. 18, No. 3, 1979, pp. 23-34

19. Schwarztrauber, P. N. and R. A. Sweet, "Efficient Fortran Subprograms for the Solution of Separable Elliptic Partial Differential Equations," *ACM Trans. Math. Software*, vol. 5, No. 3, 1979, pp. 352-364
 20. Rae Jr., W. H. and A. Pope, *Low Speed Wind Tunnel Testing*, 2nd ed., John Wiley & Sons, New York, 1984
 21. Tinoco, E. N., "CFD Applications to Complex Configurations: A Survey," in *Applied Computational Aerodynamics*, vol. 125 of *Progress in Aeronautics and Aeronautics*, AIAA, 1990, pp. 559-584
 22. Brune, G. W. and T. H. Hallstaff, "Wing Span Loads of Complex High-Lift Systems from Wake Measurements," *Journal of Aircraft*, vol. 22, No. 9, September 1985, pp. 831-832
 23. Brune, G. W. and P. W. Bogataj, "Induced Drag of a Simple Wing from Wake Measurements," SAE Paper 901934, October 1990
 24. Hallstaff, T. H. and G. W. Brune, "An Investigation of Civil Transport Aft-Body Drag Using a Three-Dimensional Wake Survey Method," AIAA Paper 84-0614, March 1984
-

